JOURNAL OF MATERIALS SCIENCE 37 (2002) 481–487

Morphological aspects of competitive grain growth during directional solidification of a nickel-base superalloy, CMSX4

N. D'SOUZA*, M. G. ARDAKANI, A. WAGNER‡, B. A. SHOLLOCK, M. McLEAN
Department of Materials, Imperial College of Science, Technology and Medicine, Prince Consort Road, London SW7 2BP, UK
E-mail: m.ardakani@ic.ac.uk

Quenched directional solidification of specially oriented bi-crystals of the Ni-base superalloy CMSX4, was carried out in an attempt to understand the role of the dendritic morphology in the process of competitive grain growth. For the range of misorientations considered (primary ⟨001⟩ misoriented by up to 7° from the uniaxial thermal gradient), there was no evidence of overgrowth of the primary misoriented dendrite by the secondary arms on the leading aligned primary. In fact, it was observed that for this range of misorientations, the tip of the retarded primary suppresses the growth of secondaries on its leading neighbour. This subsequently simply restricts the growth of the mis-aligned crystal to its original boundary, rather than reducing its size and is suggested as a possible reason for the range of stable axial orientations encountered during directional solidification of CMSX4.

1. Introduction

Directional solidification of highly alloyed second generation nickel-base superalloys, such as CMSX4, to produce turbine blades for modern aero-engines and land-based gas turbines for power generation can produce a wide range of axial orientations, often deviating from ⟨001⟩ by up to 12 to 15°, despite the solidification front being essentially planar [1–3]. This behaviour differs from the narrow range of orientations produced in earlier simpler single crystal superalloys and from the expectation from studies on model systems.

The classical grain selection mechanism proposed by Walton and Chalmers [4] is based on the difference in undercooling of favourably and unfavourably oriented dendrites with respect to the local thermal gradient, G. The favourably oriented dendrite leads and blocks its off-axis neighbour by the propagation of secondary and tertiary dendrite arms. *In situ* experiments of Huang and Glicksman [5] using a transparent organic alloy and recent studies by Ardakani *et al*. [1] on nickel-base superalloys have confirmed the fast-growing dendritic orientation to be ⟨001⟩. This is the case in most cubic systems and is consistent with the anisotropy of the solid-liquid interfacial energy, although exceptions do exist [6].

The range of orientations produced during directional solidification depends directly on the efficiency of the competitive grain growth mechanism. In the model of Walton and Chalmers [4] this is related to:

1. The difference in undercooling, which determines the distance between the tips of the leading dendrite and its lagging neighbour, and
2. The development of secondary arms on the leading dendrite ahead of the tip of the lagging dendrite.

Overgrowth of the lagging dendrite can occur by a combination of physical blocking of the misoriented dendrite or by enrichment/depletion of the solute depending on the nature of partitioning that subsequently retards its growth.

Previous studies on both metallic and transparent alloys have shown that the first secondary arms appear a short distance (d) behind the primary tip [1, 5]. In CMSX4, d was measured to be $\approx 81\ \mu$m; this would allow only small misorientations from ⟨001⟩ ($\Phi < 7°$) to grow without encountering secondary dendrites from the well-aligned orientation [1]. Larger misorientations would be expected to be overgrown.

The purpose of the present study is to clarify the mechanisms controlling the solidification texture in CMSX4 by observation of the interaction between dendrites in seeded bi-crystals of controlled misorientation. It uses a combination of quenched directional solidification and detailed microstructural characterisation on specified crystallographic planes to: (a) relate the misorientation of the off-axis dendrite to the difference in undercooling between the leading and lagging tips

* *Present Address*: Precision Casting Facility (PCF), Rolls-Royce plc, Derby DE24 8BJ, UK.
‡ *Present Address*: ALSTOM Ltd., Department GTOB-M, CH-5405 Baden-Daettwil, Switzerland.

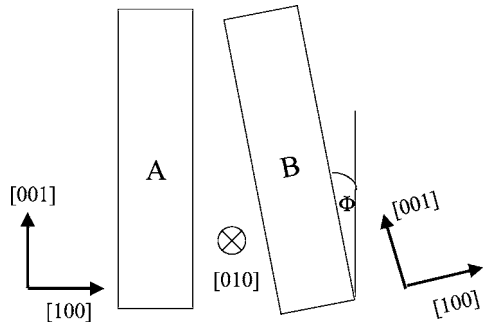

Figure 1 Schematic diagram showing spatial orientation of the bi-crystal seeds.

(i.e. the distance that the tip of the well aligned dendrite leads its off-axis neighbour), (b) determine the position where secondary arms develop on both on the leading and the lagging primary dendrites, and (c) establish the role that secondary dendrite arms play in the competitive growth process.

2. Experimental

The dendrite morphology in CMSX4, as in most face-centred cubic alloys, consists of a primary growth direction parallel to [001] with secondary arms developing in the other cube directions, [010] and [100]. To simplify microstructural analysis, a bi-crystal was produced by directional solidification in which the two grains had a common transverse [010] direction. Laue Back reflection was used to accurately position the two seeds. They were aligned as in Fig. 1; Grain A was oriented with [001] parallel to the macroscopic growth direction, while in Grain B the [001] deviated by 5 to 7° from the solidification direction.

The bi-crystal, in the form of a 6 mm diameter cylindrical ingot, was produced by the Bridgman crystal growing technique in an atmosphere of flowing argon, using a graphite susceptor and partially melting-back the seed crystals to control the orientation of the bicrystal produced. Details of the apparatus and procedures used have been described elsewhere [2]. Solidification of the bi-crystal was interrupted by quenching the ingot in a liquid metal bath. The temperature gradient (G) at the solidification front measured using R-type Pt-Pt-13%Rh thermocouples was $5 \pm 2\,\mathrm{K\,mm^{-1}}$ in agreement with a previous study [2].

The ingot was sectioned along the (010) plane common to the two crystals and through the maximum diameter of the casting. Detailed three-dimensional characterisation of the dendrite positions and morphologies in Grains A and B, with particular emphasis on their interaction where the two grains abut, was carried out by sequential mechanical and electro-polishing through the diameters of individual dendrites. The electropolishing solution was 45% 1-Butanol, 45% Acetic acid and 10% Perchloric acid by volume.; microstructural features were exposed by an etchant comprising 33% Acetic acid, 33% Nitric acid, 33% water and 1% Hydrofluoric acid by volume. The apparent positions of the dendrite tips were determined and plotted as a function of the dendrite diameter on the polished section in the course of sequential polishing steps; the position at the maximum observed dendrite diameter was taken as the true position of the dendrite tips.

3. Results

3.1. Undercooling of primary dendrite tip in directional solidification

The quenched solid/liquid interface was essentially planar and the average length of the mushy zone, from dendrite tips to eutectic pools, was measured to be 8.5 mm. The primary dendrite tips have been indicated on the longitudinal section in Fig. 2 and the fine scale of microstructure ahead of the tips corresponds to the quenched liquid. The distance between the dendrite tips in crystals A and B (designated H), measured on several longitudinal sections following sequential polishing was, $H \approx 110 \pm 14\,\mu$m (Fig. 2).

The difference in undercooling between the dendrites in the two grains can be expressed:

$$\Delta T_B - \Delta T_A = GH \tag{1}$$

where G is the thermal gradient at the solidification front and H is the distance that the leading tip is ahead of its lagging neighbour. $G = 5 \pm 2\,\mathrm{K\,mm^{-1}}$ and $H = 110 \pm 14\,\mu$m gives:

$$\Delta T_B - \Delta T_A = 0.55 \pm 0.28K \tag{2}$$

In practice, in order to satisfy energy conservation, G and G_{av} are related:

$$\Delta H_F V\rho + k_L G < k_S G_{av} \tag{3}$$

where ΔH_{F} is the latent heat per unit mass, k is the thermal conductivity, G_{av} is the average thermal gradient in the mushy zone and the subscripts s and l refer to the solid and liquid respectively. Using the physical constants for Ni-base superalloys [7] and the processing conditions ($G \approx 5\,\mathrm{K\,mm^{-1}}$, $V \approx 10^{-5}\,\mathrm{ms^{-1}}$), the latent heat contribution is ~10% of the total heat flux; also $k_L < k_S$. Therefore to the accuracy allowed by the present measurements: $G \approx G_{av}$. In fact, G_{av} determined from the present measurements of the solidification range and mushy zone length ($4.5\,\mathrm{K\,mm^{-1}}$) compares reasonably well with that determined from direct temperature measurement ($3–7\,\mathrm{K\,mm^{-1}}$). Both are consistent with previous correlations of primary dendrite arm spacing with solidification conditions [2].

3.2. Dendrite morphology and the evolution of secondary dendrite arms

Dendrites of Crystal A, remote from Crystal B, at the quenched interface show the classical morphology with the first secondary dendrite appearing $81 \pm 2\,\mu$m behind the dendrite tips. This is in agreement with previous observations [8].

Fig. 3a–c are light optical micrographs showing abutting dendrites of Crystals A and B on consecutive stages

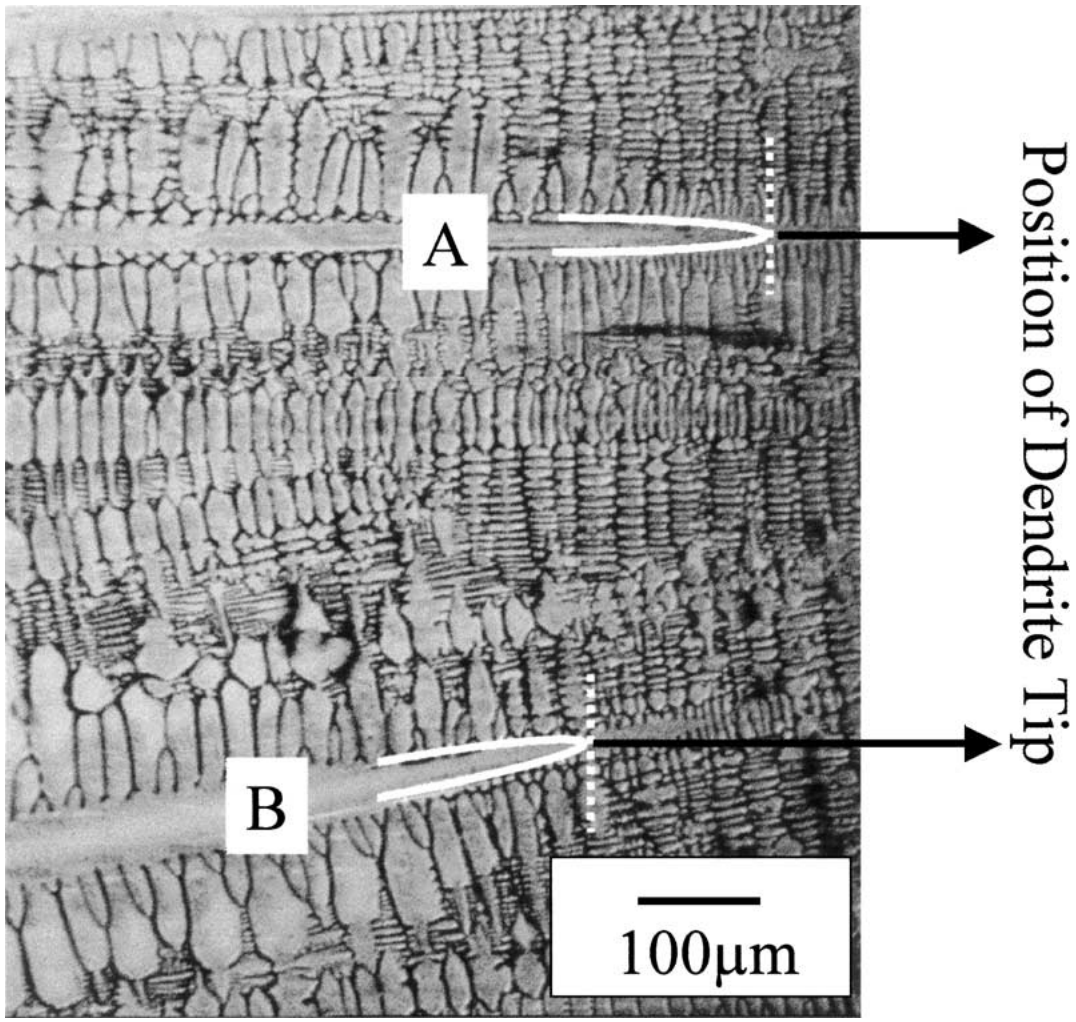

Figure 2 Light optical micrograph showing relative position of the dendrite tips of Crystals A and B after quenched directional solidification ($G = 5 \pm 2$ K mm^{-1}, $V = 2.7 \times 10^{-5}$ ms^{-1}).

of sequential polishing and imaging. The section observed is normal to the common [010] direction of the two crystals. The dendrites of Crystal A are aligned parallel to the uniaxial heat flux (thermal gradient, G), while those of Crystal B are inclined to G by an angle Φ of 5 to 7°. The following features are apparent:

(a) In Fig. 3a the core of the dendrite in Crystal A is not apparent, but the secondary dendrites parallel to [010] growing from the primary below the surface are clearly seen. The primary dendrite of Crystal B is clearly imaged showing the growth of [010] secondaries into the bulk of Crystal B, but no [100] secondaries over a length of 350 μm in the direction of Crystal A.

(b) As the specimen surface is progressively polished and imaged in Fig. 3b and c, the core of the primary dendrite in Crystal A is exposed. This also shows the development of [010] dendrites growing into Crystal A, but the absence of [100] secondaries at the intersection with Crystal B. At the same time, the primary dendrite of Crystal B is polished through exposing well-developed [010] secondaries.

(c) A second set of abutting dendrites of Crystals A and B are shown in Fig. 4a and b. In the first case, the primary dendrites appear on the same plane. It is quite apparent that the growth of secondary [100] dendrites in both crystals has been suppressed at the boundary between the misoriented crystals.

(d) The low magnification micrograph shown in Fig. 5 indicates the spacing of primary dendrites in the off-axis Crystal B that abut and are overgrown by the axially-aligned dendrites in Crystal A. It is clear that the growth of the mis-aligned dendrites ceases when they physically impinge on the cores of primary dendrites in Crystal A. There is no direct evidence of overgrowth by secondary dendrites in Crystal A blocking the growth of the mis-aligned primaries in Crystal B. The distance (D), measured parallel to the macroscopic solidification direction, of successive overgrown primary dendrites of Crystal B was $\approx 2050 \pm 8$ μm.

4. Discussion

4.1. Undercooling of primary dendrite tips

The *in-situ* solidification studies of Huang and Glicksman [5] on the transparent organic alloy succinonitrile have provided direct measurements of important physical parameters, such as the primary dendrite tip radius (R) and undercooling (ΔT). Recent measurements of dendrite tip radius, using quenched directional solidification for a range of solidification conditions by Wagner [8], has shown that the dendrite tip radius in nickel-base superalloys is at least an order of magnitude smaller

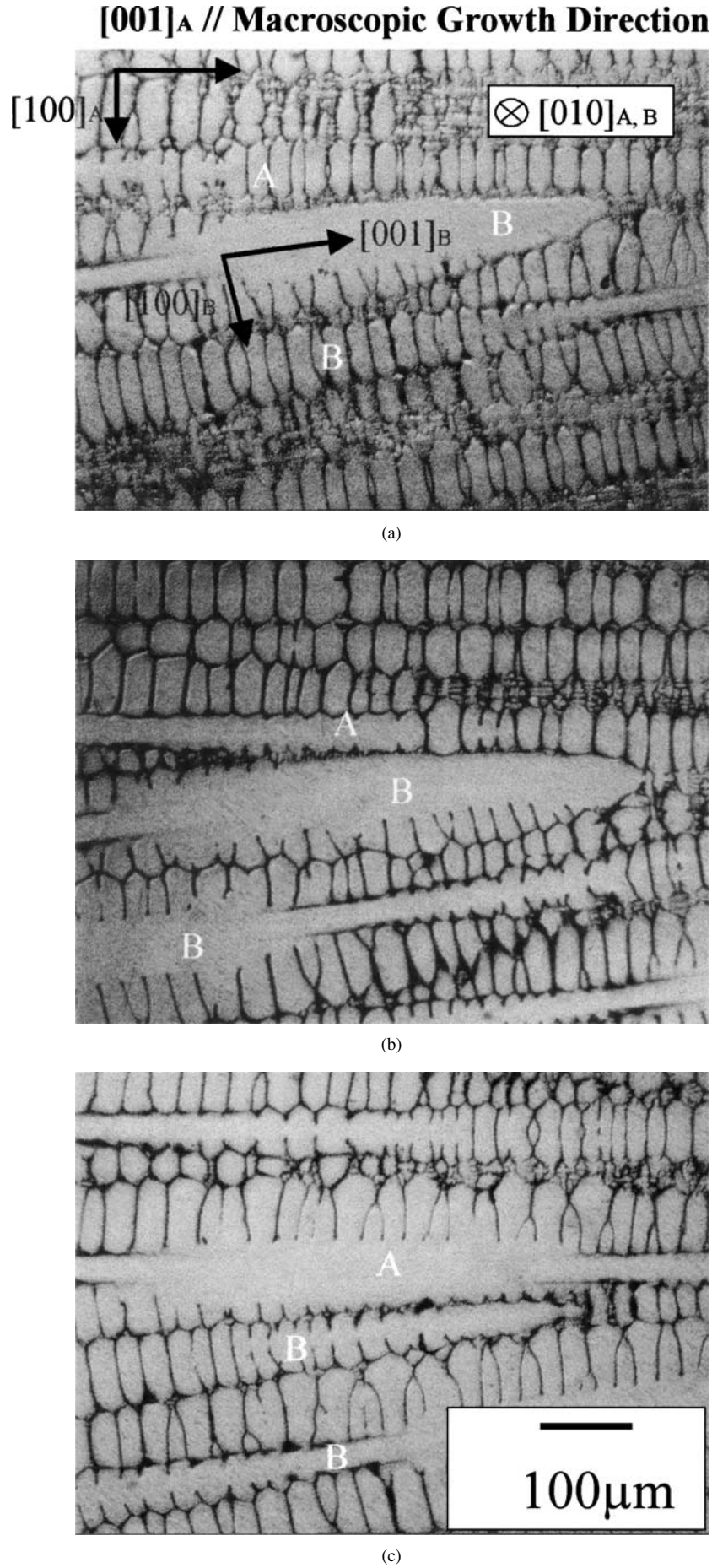

(a)

(b)

(c)

Figure 3 (a)–(c) Light optical micrograph through a series of sequential polishing showing the asymmetric evolution of [100] secondary dendrite arms when the primary dendrites of neighbouring crystals abut.

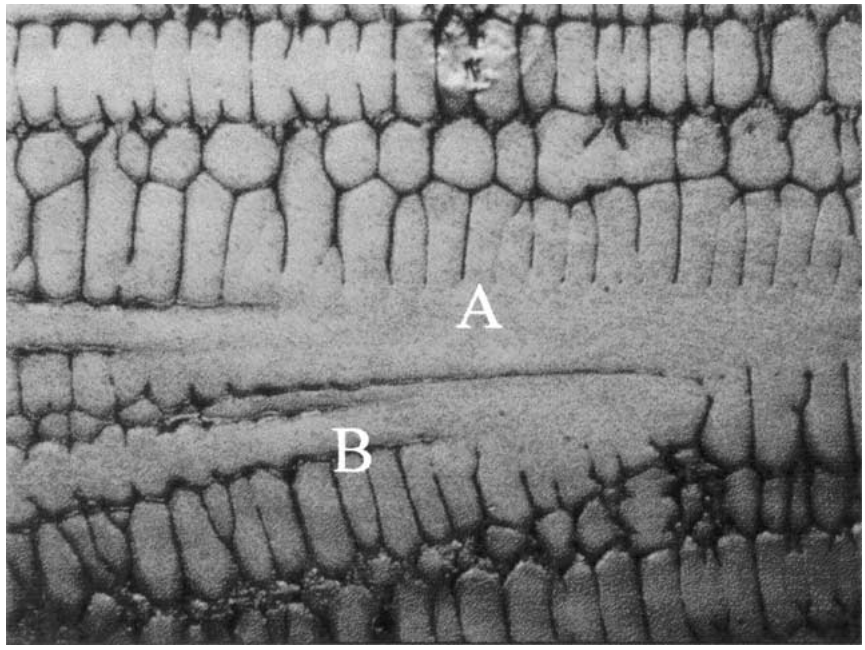

(a)

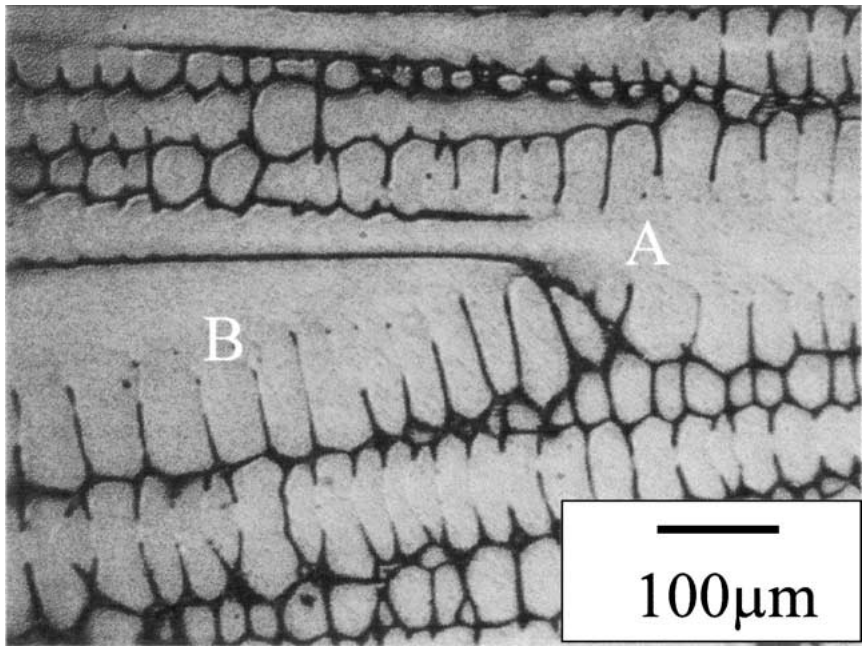

(b)

Figure 4 (a) and (b) Light optical micrograph through a series of sequential polishing showing impingement of the axial and off-axial primary stem at the crystal boundary.

than that in succinonitrile; this is comparable to the values reported by Yu *et al*. [9] for directional solidification of Pb-5.8wt% Sb. Specifically, in CMSX4 for the present solidification conditions, $R \approx 3$–8 μm [1]. It should be noted that in the present experiments on directional solidification of nickel-base superalloys, constitutional supercooling is pre-dominant, whereas in the experiments on succinonitrile, the dendrites were "free growing".

It is not possible to locate the local solidification front in quenched directional solidification experiments on opaque specimens from a single longitudinal section. This is because a random section is unlikely to pass through the precise axes of the primary dendrites; rather it will provide an off-axis section of the dendrite showing apparent values of tip radius and tip undercooling that are significantly greater than the actual values. The present experiments on carefully oriented bi-crystals and using sequential polishing and imaging have minimised these uncertainties allowing the three-dimensional morphology of the dendrites and the solidification front to be deduced. The distance between the dendrite tips of the [001] and off-[001] crystals can be determined with some precision (110 ± 14 μm for a misorientation of 5 to 7 degrees); the major uncertainty in the difference in undercooling (0.55 ± 0.28 μm) is due to errors associated with measuring the temperature gradient.

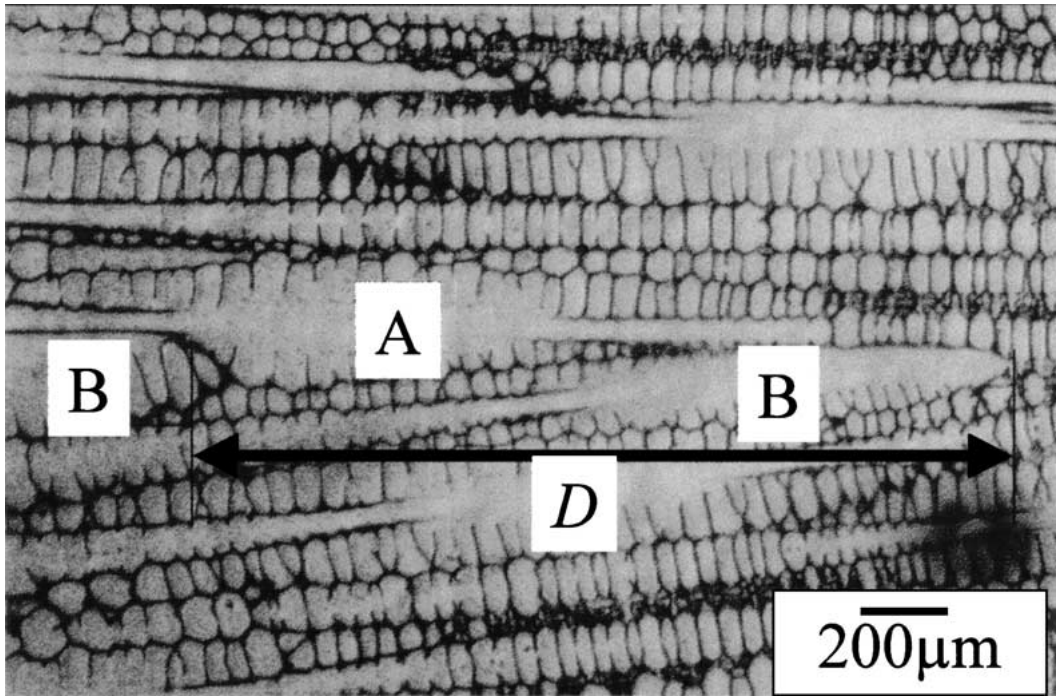

Figure 5 Light optical micrograph showing the distance along the solidification length corresponding to the overgrowth of 2 successive primary dendrites of the off-axial crystal B.

4.2. Development and suppression of secondary dendrite arms

The present experiments show that secondary arms develop from 81 μm behind the dendrite tips in Crystal A, which has [001] parallel to the temperature gradient. However, the dendrite tips in Crystal B, which has [001] inclined at 5 to 7 degrees to G, grow 110 μm behind those in Crystal A. The simple mechanism of secondary dendrites of stable orientations blocking the growth of primary dendrites of unfavorably oriented grains would predict that Crystal B should be unstable and be overgrown by Crystal A. This is not observed; Crystals A and B continue to coexist growing in parallel to produce a bi-crystal.

Where dendrites of adjacent crystals approach each other, the secondary dendrites are seen to develop in an asymmetric manner. The secondaries on dendrites in Crystals A and B grow freely into their own crystal environments. However, they do not grow readily towards the neighbouring crystal. There is clearly competition for solute between the secondaries on the advanced, well-aligned crystal and the primary dendrite of the retarded, misaligned crystal; the development of the secondaries is suppressed and the mis-aligned primary continues to grow until it physically encounters the aligned dendrite. This simply restricts the growth of the mis-aligned crystal to its original boundary, rather than reducing its size. The distance between arrested dendrites of Crystal B along the ingot length (D) is a simple geometrical function of the misorientaton (Φ) and the primary dendrite arm spacing (Λ):

$$\tan \Phi = \frac{\Lambda}{D} \tag{4}$$

Λ was measured as 213 ± 18 μm in the present experiments and combining this with $\Phi = 5$–7 degrees gives a range of D ($D \sim$ 1735–2434 μm), which is comparable to the measured value of 2050 μm.

The present experiments clearly show that at the boundary between two growing crystals, there is a significant interaction between the neighbouring dendrites that influence the development of secondary arms. Consequently, the normally accepted mechanism of overgrowth of misoriented crystals by the development of secondaries and tertiaries originating from fast growing orientations must be modified to account for the suppression of secondary growth by the retarded primary dendrites. This means that a wider range of orientations can grow in a stable manner, than would be expected from a knowledge of the average dendrite morphology. A quantitative mechanism of competitive grain growth must incorporate this suppression of secondary dendrites.

The sharpness of texture produced by directional solidification of nickel-base superalloys has been shown to be sensitive to the alloy chemistry. The introduction of highly segregating refractory elements (e.g. rhenium, tungsten) in second and third generation single crystal superalloys has been accompanied by a wider range of orientations being produced than for first generation alloys. There is no significant difference in the morphologies of dendrites remote from boundaries for these alloys. It is likely that local distortions to the dendrite morphology due to competition for the solute may be the cause of these differences. The present experiments are being extended to a wide range of orientations and to different alloys to clarify the criteria for competitive grain growth.

5. Conclusions

1. The difference in undercooling of dendrites aligned parallel and at an angle Φ ($5^\circ \leq \Phi \leq 7^\circ$) to the local

thermal gradient was 0.55 ± 0.28 K for a solidification rate of 2.7×10^{-5} ms^{-1}.

2. Although the primary mis-aligned dendrites are retarded relative to the initiation of secondaries on the well-aligned dendrites, there is no evidence of overgrowth of the mis-oriented grain by these secondaries.

3. The tip of the retarded primary dendrite distorts the solute field ahead of it and suppresses the growth of secondary dendrites on the adjacent favorably oriented crystal allowing the retarded crystal to grow in a stable manner.

4. An effective competitive grain growth mechanism must incorporate this solute interaction effect, which is likely to be sensitive to the detailed alloy chemistry.

Acknowledgements

The authors thank ALSTOM ENERGY (formerly European Gas Turbines) for provision of a studentship (ND's) and EPSRC for support (Grant No. GR/L05433).

References

1. M. G. ARDAKANI, N. D'SOUZA, A. WAGNER, B. A. SHOLLOCK and M. MCLEAN, in "Superalloys 2000," edited by T. M. Pollock, R. D. Kissinger, R. R. Bowman, K. A. Green, M. McLean, S. L. Olson and J. J. Schirra (TMS, Minerals, Metals, Materials) p. 219.
2. N. D'SOUZA, M. G. ARDAKANI, M. MCLEAN and B. A. SHOLLOCK, *Metall. Mat. Trans.* **31A** (2000) 2877.
3. P. CARTER, D. C. COX, CH.-A. GANDIN and R. C. REED, *Mat. Sci. and Eng.* **A280** (2000) 233.
4. D. WALTON and B. CHALMERS, *Trans. Metall. Soc. AIME* **215** (1959) 447.
5. S-C. HUANG and M. E. GLICKSMAN, *Acta Met.* **29** (1981) 717.
6. D. N. LEE, K.-H. KIM, Y. LEE and C.-H. CHOI, *Materials Chemistry and Physics* **47** (1997) 154.
7. T. J. FITZGERALD and R. F. SINGER, *Met. and Mat. Trans.* **28A** (1997) 1377.
8. A. WAGNER, unpublished research.
9. L. YU, G. L. DING, J. REYE, S. N. OJHA and S. N. TEWARI, *Metall. and Mat. Trans.* **30A** (1999) 2463.

Received 17 April
and accepted 3 August 2001